CRYSTAL SELECTION AND LIESEGANG BANDING IN DYNAMIC PRECIPITATE SYSTEMS

Shoghag PANJARIAN[1] and Rabih SULTAN[2,*]

Department of Chemistry, American University of Beirut, Beirut, Lebanon;
e-mail: [1] shogh_bp@hotmail.com, [2] rsultan@aub.edu.lb

Received November 30, 2000
Accepted March 13, 2001

We report on some phenomenological properties of precipitate patterns grown in gels. The experiments span a variety of salt systems, and yield patterns ranging from Liesegang bands to exotic crystals and to a combination of both depending on the initial conditions. The obtained crystals encompass spots, crystallites and notably dendrites of fractal nature. The particle number and size observed in discrete spotted bands of a cobalt oxinate Liesegang pattern provide a direct verification of Ostwald ripening.

Keywords: Liesegang; Periodic precipitation; Crystal growth; Ostwald ripening; Dendrites; Lead fluoride; Lead iodide; Chromium fluoride; Cobalt oxinate.

Precipitation and crystal growth in gel media[1] are gaining increasing interest because of potential applications in a variety of fields notably in geology[2,3]. Precipitate systems are transiently out of equilibrium and their evolution obeys nonlinear dynamic equations[4]. Periodic banding (often known as Liesegang[5] banding) arises when co-precipitate solutions interdiffuse in a gel medium.

Certain experiments performed under similar conditions fail to give band stratification but could yield other interesting structures such as a propagating single precipitate band[6,7], uniform precipitation zones[8], or a variety of crystals. A propagating stratum of bands was also observed[7,9] in some systems. The literature also presents a variety of instances where Liesegang bands themselves consist of macroscopic crystals visible with a naked eye. A diverse morphology of crystals can be obtained, either as an alternative to the Liesegang bands or as components of those bands on a smaller scale. In early studies, Hatschek[10] pointed out that even when good Liesegang rings are formed, they are not necessarily the only reaction product. He carried out a study of the particle size distribution in a variety of Liesegang bands.

In the present paper, we report a variety of precipitate patterning experiments (of the Liesegang type), wherein we obtain different character-

istic crystal shapes in a typical reproducible manner. The purpose of the study is to explore the variety of patterns obtained with an emphasis on the type of crystals selected by the dynamics under specific experimental conditions. The crystals range from spots to crystallites to dendrites (tree-like aggregates). Liesegang bands are also obtained of either compact nature or themselves consisting of distinct crystal shapes such as spots or crystallites. In each salt system studied, we draw a comparison between our experiments and related findings in the literature with similar patterning structures, with an emphasis on dendrites, their nature and their characterization. A classification of the various morphologies obtained is finally summarized and tabulated in the conclusion.

Spots, Dendrites and Liesegang Bands in PbF_2 Systems

Experimental

A solution containing one of the co-precipitate ions (Pb^{2+} or F^-) at the desired concentration with 1% agar (Difco, bacto-agar) is heated to 90 °C with constant stirring for about 5 min. The mixture is then poured into thin tubes of 5.0 mm diameter and allowed to cool until the gelation is complete (about 2 h). A solution containing the other ion is poured on top of the solidified gel. The range of concentrations used for both the upper and lower solutions in the various experiments is indicated in Table I. Parallel

TABLE I
Domains of Pb^{2+} and F^- initial concentrations, where the various types of PbF_2 crystals are obtained (❐ spots, ◆ spots and dendrites, ● big dendrites, Δ small dendrites, ★ intermediate size dendrites)

$[Pb^{2+}]_0$, mol/l	$[F^-]_0$, mol/l								
	0.81	0.90	1.00	1.35	1.50	1.80	2.00	3.00	4.00
0.090	❐	❐	❐	❐	❐	❐	❐	❐	❐
0.10	❐	❐	❐	❐	❐	❐	❐	❐	❐
0.20	❐	❐	❐	❐	❐	❐	❐	❐	❐
0.30	◆	◆	◆	◆	◆	◆	◆	◆	◆
0.45	●	●	●	●	●	★	Δ	Δ	Δ
0.50	●	●	●	●	●	★	Δ	Δ	Δ
0.60	●	●	●	●	●	★	Δ	Δ	Δ

bands or crystals of white PbF_2 (depending on the conditions as discussed below) start appearing within 1 h. In another set of experiments, the above procedure is repeated in a gel layer (of thickness 2 mm) sandwiched between two parallel microslides to allow a convenient observation under the microscope. The slides are sealed with silicone and the hot gel solution is poured into the space between them similarly as for the tubes (filling up to a level of 2/3 the slide length). After around 1 h necessary for gelation, the upper solution is poured on top of the gel.

Results and Discussion

Two major classes of patterns are obtained. When the lower (gel) solution contains the anion (F^-) and the upper solution the cation (Pb^{2+}), distinct Liesegang bands are obtained, displayed in Fig. 1. A wide range of concentrations of the two ions was tested. In all cases, Liesegang bands were clearly observed.

A rich variety of phenomena is obtained when the roles of the electrolytes are reversed (*i.e.* Pb^{2+} in lower solution, F^- in upper solution). Instead of getting bands, three categories of crystal selections (depicted in Fig. 2) were obtained: spots (Fig. 2a), dendrites (Figs 2c, 2d) and mixtures of both (Fig. 2b). Dendrites[11] are tree-like patterns displayed by some precipitates[12–17] and some rock minerals (most notably MnO_2 in refs[18,19]). Visible with a naked eye in some samples, and displaying similar structures at different length scales, they are scale-invariant structures and thus are clas-

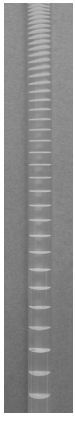

FIG. 1
Liesegang bands of PbF_2 obtained when a Pb^{2+} solution diffuses into an agar solution of I^-. The bands are clearly defined and the pattern is very stable

sified as fractal objects[20]. Note that reversing the roles of the electrolytes in Pb^{2+}/I^- interdiffusion experiments (precipitating PbI_2) by Müller *et. al.*[21], also gave Liesegang bands and did not yield the crystalline geometries encountered here for PbF_2. A coexistence between periodic precipitation and tree-like aggregates in PbI_2 systems was however reported in a special experiment by Toramaru *et al.*[14].

Figure 2 shows pictures of the various crystal displays obtained in tubes. Note that two types of dendrites are noticed: big and small. The small dendrites have a leaf-like structure but are independent entities (Fig. 2c), while big dendrites are linked through a spatial network resembling a real tree with complex branching (Fig. 2d). Table I summarizes the results obtained, by showing the various domains in the $[F^-]_0/[Pb^{2+}]_0$ phase space where each of the three categories is observed (the subscript 0 denotes initial concentrations).

We can see that there exists a critical initial lead ion concentration ($[Pb^{2+}] \approx 0.3$ mol/l) below which no dendrite formation is seen. The distinction between big and small dendrites is established by going horizontally through the dendrite domains, *i.e.* by increasing $[F^-]_0$ through the value 1.8 mol/l. Thus we can see that the transition from spots to dendrites (and *vice versa*) is a vertical transition and not diagonal in the $[F^-]_0/[Pb^{2+}]_0$ phase space. An alternative approach is to examine the various domains of crystal selection as the concentration difference (Δ) and the ion product (σ), introduced by Müller *et al.*[21] defined by

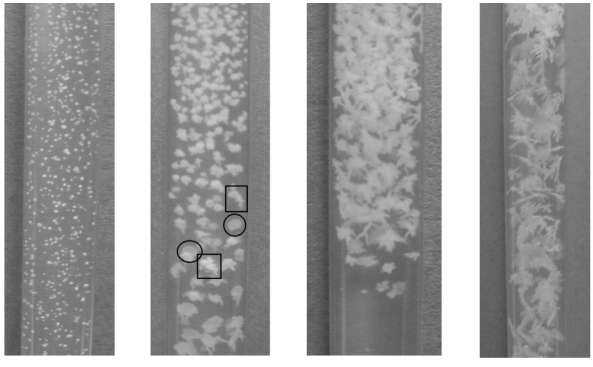

FIG. 2
Crystal selection of PbF_2 in various domains of Pb^{2+} and F^- concentrations whose topology is detailed in Table I. The experiments here involve the diffusion of F^- (upper solution) into a Pb^{2+} gel: a spots, b spots and dendrites, c small dendrites, d big dendrites

$$\Delta = \frac{1}{2}[F^-]_0 - [Pb^{2+}]_0 \qquad (1)$$

and

$$\sigma = [Pb^{2+}]_0 [F^-]_0^2 \ , \qquad (2)$$

are varied (note that in the units of the solubility product σ_0, σ can be taken as the initial supersaturation in the tubes). The results are depicted in the plot of Fig. 3. The solid line represents the borderline situation where both spots and dendrites are obtained in the same experiment (observed in the same tube, as seen in Fig. 2b). Thus we see that using the Δ and σ variables, we obtain a nearly diagonal transition between spots and dendrites. Figure 4 shows dendrites like the ones of tube 2d but grown in a gel sandwiched between two microslides, to allow a convenient observation under the microscope. An experimental procedure exactly similar to the one for the tubes was followed. Figure 5 shows microphotographs highlighting details of both the spot patterns and the dendritic tree-like PbF_2 structures.

Thus we see that various types of crystalline PbF_2 patterns can be obtained selectively by a mere convenient choice of the initial concentrations

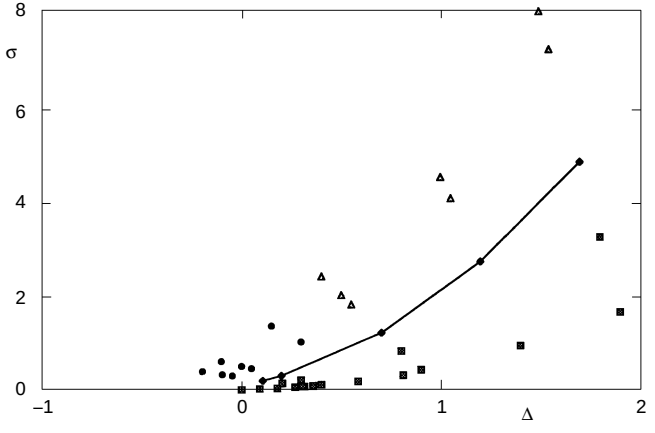

FIG. 3

Domains of Δ and σ (defined by Eqs (*1*) and (*2*)), where the various categories of crystals are obtained. The solid line delineates the borderline between the spots and the dendrites domains, joining points where both spots and dendrites (◆) are observed in the same tube (spots (■), small dendrites (Δ), big dendrites (●)). A more interesting transition than a trivial vertical one is possible with a wide choice of Δ and σ

of the inner and outer electrolytes. In a number of studies, other factors such as the concentration of gel[14], its degree of swelling, and its degree of polymer crosslinking[15] were found to control the patterning properties of various salt systems including the formation of tree-like aggregates (dendrites). Tree-like aggregates are formed *via* different chemical routes and can be characterized by standard methods[22,23]. Dendrites were observed[13] as a transient crystalline phase in PbS systems between an initial skeletal form and the known final cubic form. Büki *et al.*[16,17] showed that dendrite ramifications in $PbCl_2$/PVA gel systems obey periodic laws similar to those of the Liesegang stripes. Dendritic patterns were also reported in the electrodeposition of zinc (metal leaves)[24], the growth of succinonitrile plastic crystals[25], and solidification from undercooled melts and supersaturated solutions[26]. Sunagawa[27] proposed a qualitative model relating growth habit to supersaturation. He showed that above a critical supersaturation, the growth mechanism switches from two-dimensional to three-dimensional surface nucleation resulting in dendrite formation. Chopard *et al.*[19] showed that mineral dendrites (such as those of manganese oxides) are driven by a lattice reaction-diffusion dynamics. Calculated fractal dimensions for a variety of dendritic patterns[11,19], using the sand-box counting technique[20], range from 1.51 in quartz to 1.78 in limestone[19]. The intermediate value 1.69 was also reported in some pyrolusite minerals from Spain. Two main mechanisms[28] are believed to support the formation of mineral dendrites: (i) diffusion-limited aggregation (DLA), characterized by irreversible growth

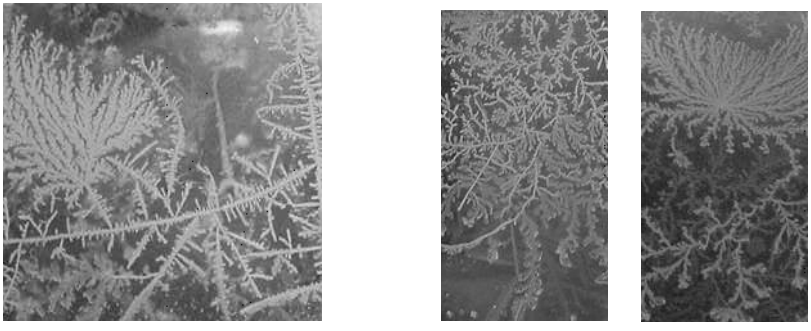

a b

FIG. 4

Tree-like (dendrite) PbF_2 patterns grown in microslides *via* a classic interdiffusion Liesegang experiment. The dendrites appear suddenly after a long time of nonexistent solid PbF_2 in a clear gel (1% agar). $[F^-]_0$ = 1.0 mol/l, $[Pb^{2+}]_0$ = 0.4 mol/l: pattern appeared after 39 days (a); $[F^-]_0$ = 1.0 mol/l, $[Pb^{2+}]_0$ = 0.3 mol/l: pattern appeared after 56 days (b)

a

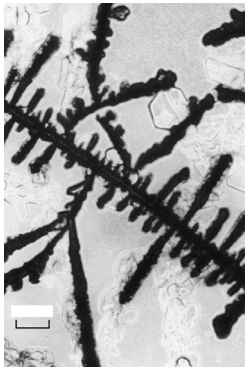

b

c

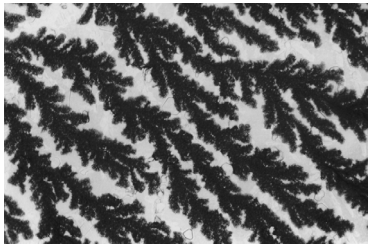

d

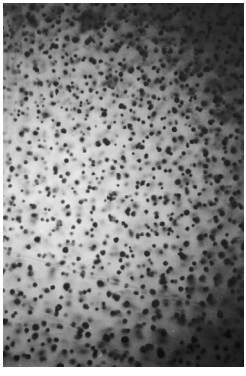

e

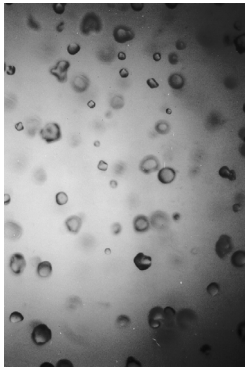

f

FIG. 5

Microphotographs of different regions of the dendritic pattern in Fig. 4a (a–d), spot patterns ($[F^-]_0$ = 1.0 mol/l, $[Pb^{2+}]_0$ = 0.1 mol/l): upper portion (e) and lower portion (f) of the sandwiched gel. Fewer and larger crystals are observed near the bottom as explained in Section Spotted Liesegang Bands in Cobalt(II) Oxinate Systems and also in the caption of Fig. 8

processes governed by the diffusional control of the nutrient phase and (ii) viscous fingering (VF) created when one fluid pushes another of higher viscosity. Viscous fingering in porous media and percolation were treated and explained form the viewpoint of fractal geometry[29]. García-Ruiz *et al.*[11] proposed a self-fed mechanism whereby a certain fluid invades a more viscous fluid medium by injection through cracks. They simulated the mechanism in a laboratory experiment wherein fractures (like cracks in a rock) were provoked by hammering a pile of glass disks hosting the medium. A full characterization of the PbF_2 dendrites obtained in this work (including the calculation of fractal dimension) is the subject of the following paper.

Random Crystallites

In some salt systems, Liesegang bands are themselves made up of dispersed crystals showing an internal structure within the overall stratification. Needles could constitute the morphology of Ag_2CrO_4 bands[1], while granules make up some bands in a single-salt[30] ($Ca_3(PO_4)_2$) and two-salt[31] (PbI_2/PbF_2) systems. In this section, we report on some experiments that yield clear randomly distributed crystallites. A crystallite is defined as an aggregate of small crystals appearing as a homogenous elongated precipitate zone of random shape and location.

CrF_3 Liesegang Experiments

A 1% agar solution is heated to 90 °C with constant stirring for about 1 min. Then solid $Cr(NO_3)_3 \cdot 9H_2O$ is added with continued heating and stirring for another 4 min. The mixture is then poured into a 6.0 mm diameter tube and allowed to cool until the gel solidifies. A KF solution is added on top of the gel after about 1 h. The concentrations used are given in the caption of Fig. 6. CrF_3 precipitates out gradually in the gel as both spots and crystallites in a random manner covering about a 4 cm distance below the interface. After this chaotic regime, the spots and crystallites continue to appear, but arranged in stratified zones (bands) like in a classic Liesegang pattern. Figure 6a shows a picture of a typical CrF_3 pattern obtained in tubes. Figure 6b shows the details under the microscope. A mixture of both spots and crystallites is observed. Liesegang bands themselves made up of small crystallites appear at a late stage of the pattern evolution (see the first band at the bottom of the pattern in frame a and the development of more bands in Fig. 6c).

Crystallites and Coarsening in Supercooled PbI_2 Experiments

We use here a procedure[32,34] different from that of the classic Liesegang experiment. A 0.25 g sample of agar (Difco, bacto-agar) is weighed to the nearest 0.01 g and transferred to a double-neck round-bottom flask fitted with a condenser and containing 100.00 ml of distilled water. The agar solution is heated under reflux with gentle stirring until the temperature reaches 98 °C. Then, an accurately weighed sample (0.200–0.240 g) of lead iodide is added. The flask is kept under reflux for 30 min during which the solution remains relatively clear (PbI_2 is soluble at high temperature). The mixture is then poured into a pre-heated test tube and the latter sealed with parafilm paper. As the solution cools down (within about 30 min), a uniform yellow haze of precipitate is formed, which then breaks up into precipitate zones separated by clear (precipitate free) domains. The precipitate zones appear mainly as randomly distributed crystallites of variable sizes (depending on the concentration) embedded in the gel.

Five tubes with five different initial PbI_2 concentrations (c_0) are prepared. The results are depicted in Fig. 7. We can see that a higher initial concentration results in a pattern of a lower wavelength, *i.e.* a more coarsened precipitate distribution. The transition is from small crystals (frame a) to large isolated crystallites (frame b) to a network of linked crystallites (frame c) to

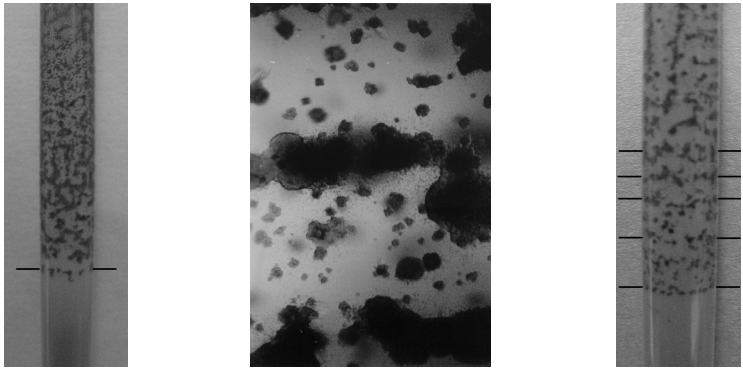

FIG. 6

CrF_3 pattern consisting of spots and crystallites ($[F^-]_0$ = 3.0 mol/l, $[Cr^{3+}]_0$ = 0.25 mol/l) (a). Portion of the pattern in frame a seen under the microscope; the spots and the crystallites are clear and distinct (b). Liesegang bands (indicated with short lines on both sides of the tube) with crystallite structure forming at a late stage of the pattern evolution (c). The wake of the first band is seen in frame a

gradually coarsening homogeneous precipitates (frames d and e). Those spatially inhomogeneous patterns formed without imposed concentration gradients resemble the two-dimensional speckled patterns (in Petri dishes) of Feinn *et. al.*[32] and Kai *et al.*[33]. In the latter work, the pattern wavelength ranges from 0.5 to 10 mm depending on initial concentrations. The coarse patterns reproduce the experimental results of Flicker and Ross[34] (in thin pipettes). Our experiments extend those systematic observations to a three-dimensional (3D) network in large test tubes (of diameter 1.5 cm). They most notably determine a characteristic PbI_2 concentration c_0 = 4.56 mmol/l at which distinct random crystallites are observed.

A theory of competitive coarsening analyzing the various properties of pattern formation in precipitation processes, notably in the absence of concentration gradients is presented in ref.[35].

Spotted Liesegang Bands in Cobalt(II) Oxinate Systems

Ostwald Ripening

A precipitate is a large collection of small particles of different sizes which exhibits a dynamic evolution. The sizes of particles initially born obey a spatial distribution which can be expressed mathematically in different

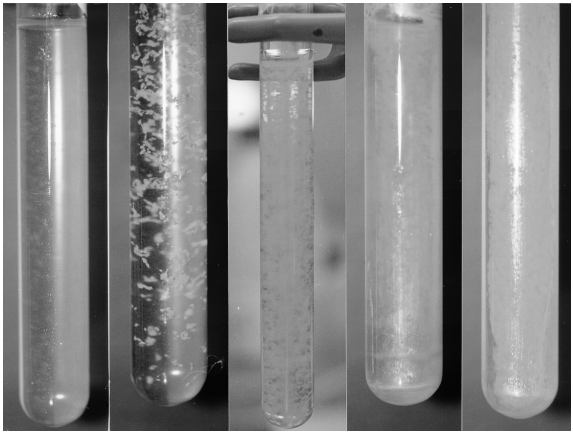

FIG. 7
PbI_2 patterns formed by cooling hot solutions of the salt with different initial concentrations. c_0 = 4.34 mmol/l: small crystals (a), c_0 = 4.56 mmol/l: large crystallites (b), c_0 = 4.77 mmol/l: network (c), c_0 = 4.99 mmol/l (d), c_0 = 5.21 mmol/l: coarsening (e)

forms, such as a small amplitude disturbance in a localized spatial position[32,35,36] or a random noise distribution[37]. Because of surface tension effects, the larger particles have a higher solubility than smaller particles; the coupling of this effect to the diffusion of the dissolved ions results in that larger particles grow at the expense of smaller ones. As a result, the system evolves with time toward a state of fewer but larger particles. This interesting phenomenon is traditionally known as Ostwald ripening[35,38]. The modeling of the competition between particle ensembles was initiated in a leading paper by Lifshitz and Slyosov[39]. While coarse bands in a precipitate require sophisticated techniques for fine particle size measurement, the choice of suitable experimental conditions allows an easy verification of Ostwald ripening in Liesegang systems by direct observation.

Cobalt(II) Oxinate Liesegang Experiments

We prepare a set of Co(II) oxinate patterns in tubes as suggested by Kanniah *et al.*[40]. 0.218 g of 8-hydroxyquinoline (oxine, Analar) are dissolved in 2.0 M acetic acid with gentle heating. Then 25% ammonia solution is added dropwise to the mixture until a faint and permanent turbidity is observed. A few drops of acetic acid are then added to dissolve the turbidity producing a solution of pH 4.1. The volume is made up to 50.0 ml with distilled water, then 0.505 g of agar (Difco) are added and the mixture is heated until the gel solution is clear. This oxine/gel solution ($[\text{oxine}]_0$ = 0.030 mol/l) is poured into thin glass tubes (diameter 4.0 mm). After gelation is complete, a 0.515 M Co^{2+} solution (prepared from $CoCl_2 \cdot 6H_2O$) is poured on top of the gel.

When the above concentrations are used, we obtain Co(II) oxinate patterns with periodic precipitate zones consisting of dispersed particles, easily distinguishable with a naked eye, as shown in Fig. 8a (coarse bands may be obtained at higher Co^{2+} concentrations). By examining the various bands, we remark that the average particle size is not uniform in all of them, but increases (on the average) with the band number, *i.e.*, as we go down the tube (see Fig. 8b). We further notice that the number of particles decreases as we go from top to bottom (Fig. 8b), *i.e.*, the bands at the bottom contain considerably less particles of larger size than the ones at the top. Those two simple observations constitute a direct verification of Ostwald ripening. A quantitative formulation of the present observations with a rigorous measurement of number of particles and average particle size within a given band, as a function of band number is under current investigation.

TABLE II
Summary of patterns, with the types of crystals obtained, in all the performed experiments

Salt system	Patterns observed	Type of experiment
PbF_2	Spots, dendrites and mixtures of spots and dendrites. Transition from one pattern to the other is controled by concentration parameters (see Table I)	Liesegang/interdiffusion F^- upper, Pb^{2+} lower
PbF_2	Liesegang bands	Liesegang/interdiffusion Pb^{2+} upper, F^- lower
CrF_3	Spots and crystallites over a 4 cm length followed (in time) by the wake of Liesegang bands made up of crystallites	Liesegang/interdiffusion
PbI_2	Randomly distributed crystallites at c_0 = 4.56 mmol/l	Supercooled
$Co(Ox)_2$	Liesegang bands made up of spots	Liesegang/interdiffusion

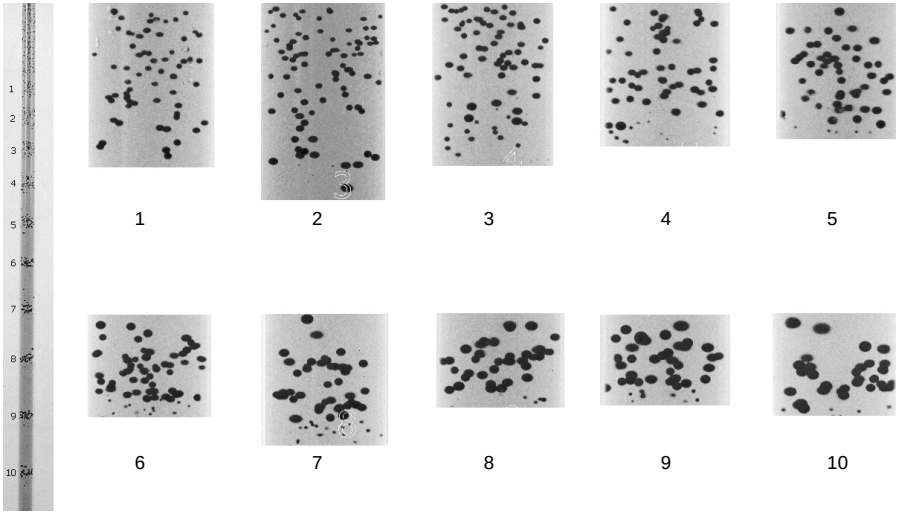

FIG. 8
Liesegang bands of Co(II) oxinate consisting of small granules (a). Enlarged pictures of the bands (labeled 1–10) in the tube of frame a (b). As the band number increases (in going from top to bottom), the average particle size in a given band increases and the number of particles decreases

Conclusions

In this study, we explored the variety of patterns obtained in precipitate systems in gels, with a special attention to the types of crystalline structure involved. A wide variety of patterns with different exotic types of crystals is obtained depending on the choice of experimental conditions. The overall results are summarized in Table II.

We can thus see a wide diversity with a clear potential for crystal selection.

This work was supported by a University Research Board, American University of Beirut (grant No. DCU17996071502). We thank Mrs S. Sadek and Miss N. Al-Kassem for their feedback in the experiments of Sections Crystallites and Coarsening in Supercooled PbI_2 Experiments and Cobalt(II) Oxinate Liesegang Experiments.

REFERENCES

1. Henisch H. K.: *Crystals in Gels and Liesegang Rings*. Cambridge University Press, Cambridge 1988.
2. Ortoleva P.: *Geochemical Self-Organization*. Oxford University Press, New York 1994.
3. Kruhl J. H. (Ed.): *Fractals and Dynamic Systems in Geoscience*. Springer-Verlag, Berlin 1994.
4. Droz M.: *Lect. Notes Phys.* **1999**, *519*, 211.
5. Liesegang R. E.: *Liesegang's photographisches Archiv* **1896**, *37* (*21*), 321.
6. Zrínyi M., Gálfi L., Smidróczki É., Rácz Z., Horkay F.: *J. Phys. Chem.* **1991**, *95*, 1618.
7. Das I., Pushkarna A., Argawal N. R.: *J. Phys. Chem.* **1989**, *93*, 7269.
8. Sharbaugh A. H., III, Sharbaugh A. H., Jr.: *J. Chem. Educ.* **1989**, *66*, 589.
9. Nasreddine V., Sultan R.: *J. Phys. Chem. A* **1999**, *103*, 2934.
10. Hatschek E.: *Kolloidn. Zh.* **1911**, *8*, 13.
11. García-Ruiz J. M., Otálora F., Sanchez-Navas A., Higes-Rolando F. J. in: *Fractals and Dynamic Systems in Geoscience* (J. H. Kruhl, Ed.), p. 307. Springer-Verlag, Berlin 1994.
12. Das I., Pushkarna A., Bhattacharjee A.: *J. Phys. Chem.* **1991**, *95*, 3886.
13. García-Ruiz J. M.: *J. Cryst. Growth* **1986**, *75*, 441.
14. Toramaru A., Iochi A.: *Kobutsugaku Zasshi* **1997**, *26*, 103; *Chem. Abstr.* **1997**, *127*, 115497.
15. Kárpáti-Smidróczki É., Büki A., Zrínyi M.: *Colloid Polym. Sci.* **1995**, *273*, 857.
16. Büki A., Kárpáti-Smidröczki É., Zrínyi M.: *Physica A (Amsterdam)* **1995**, *220*, 357.
17. Büki A., Kárpáti-Smidróczki É., Zrínyi M.: *Hung. Magy. Kem. Foly.* **1995**, *101*, 524; *Chem. Abstr.* **1996**, *124*, 127856.
18. Potter R. M., Rossman G. R.: *Am. Mineral.* **1979**, *64*, 1199.
19. Chopard B., Herrmann H. J., Vicsek T.: *Nature* **1991**, *353*, 409.
20. Mandelbrot B. B.: *The Fractal Geometry of Nature*. Freeman, San Francisco 1982.
21. Müller S. C., Kai S., Ross J.: *J. Chem. Phys.* **1982**, *86*, 4078.
22. Harrison A.: *Fractals in Chemistry, Oxford Chemistry Primers*, No. 22. Oxford University Press, Oxford 1995.
23. Barnsley M.: *Fractals Everywhere*. Academic Press, New York 1988.

24. Matsushita M., Sano M., Hayakawa Y., Honjo H., Sawada Y.: *Phys. Rev. Lett.* **1984**, *53*, 286.
25. Langer J. S.: *Science (Washington, D. C.)* **1989**, *243*, 1150.
26. Ben-Jacob E., Garik P.: *Nature* **1990**, *343*, 523.
27. Sunagawa I.: *Bull. Mineral.* **1981**, *104*, 81.
28. Viscsek T.: *Fractal Growth Phenomena*, 2nd ed. World Scientific, Singapore 1992.
29. Feder J.: *Fractals*. Plenum Press, New York 1988.
30. Hatschek E.: *Biochem. J.* **1920**, *14*, 418.
31. Attieh M., Al-Kassem N., Sultan R.: *J. Chem. Soc., Faraday Trans.* **1998**, *94*, 2187.
32. Feinn D., Scalf W., Ortoleva P., Schmidt S., Wolff M.: *J. Chem. Phys.* **1978**, *69*, 27.
33. Kai S., Müller S. C., Ross J.: *J. Phys. Chem.* **1983**, *87*, 806.
34. Flicker M., Ross J.: *J. Chem. Phys.* **1974**, *60*, 3458.
35. Venzl G.: *J. Chem. Phys.* **1986**, *85*, 1996.
36. Feeney R., Ortoleva P., Strickholm P., Schmidt S., Chadam J.: *J. Chem. Phys.* **1983**, *78*, 1293.
37. Sultan R., Ortoleva P.: *Physica D (Amsterdam)* **1993**, *63*, 202.
38. Liesegang R.: *Z. Phys. Chem.* **1911**, *75*, 374.
39. Lifshitz I. M., Slyozov V. V.: *J. Phys. Chem. Solids* **1961**, *19*, 35.
40. Kanniah N., Gnanam F. D., Ramasamy P.: *Proc. Indian Acad. Sci., Chem. Sci.* **1984**, *93*, 801.